

Anomeric and Mesomeric Effects in Methoxycarbonylsulfenyl Chloride, $\text{CH}_3\text{OC}(\text{O})\text{SCI}$: An Experimental and Theoretical Study[†]Mauricio F. Erben,[‡] Carlos O. Della Védova,^{*†§} Rosana M. Romano,[‡] Roland Boese,^{||} Heinz Oberhammer,[⊥] Helge Willner,[∇] and Oswaldo Sala[∞]

CEQUINOR (UNLP, CONICET), Departamento de Química, Facultad de Ciencias Exactas, y Laboratorio de Servicios a la Industria y al Sistema Científico, Universidad Nacional de La Plata, 47 esquina 115 (1900) La Plata, República Argentina, Institut für Anorganische Chemie, Universität GH Essen, Universitätsstrasse 5-7, D-45117 Essen, Germany, Institut für Physikalische und Theoretische Chemie, Universität Tübingen, Germany, FB 6, Anorganische Chemie, Universität GH Duisburg, D-47048 Duisburg, Germany, and Instituto de Química, Universidade de Sao Paulo, C. P. 26077, Sao Paulo, Brasil

Received July 12, 2001

The molecular structure and conformational properties of methoxycarbonylsulfenyl chloride, $\text{CH}_3\text{OC}(\text{O})\text{SCI}$, were determined in the gas and solid phases by gas electron diffraction, low-temperature X-ray diffraction, and vibrational spectroscopy. Furthermore, quantum chemical calculations were performed. Experimental and theoretical methods result in structures with a planar $\text{C}-\text{O}-\text{C}(\text{O})-\text{S}-\text{Cl}$ skeleton. The electron diffraction intensities are reproduced best with a mixture of 72(8)% syn and 28(8)% anti conformers ($\text{S}-\text{Cl}$ bond synperiplanar/antiperiplanar with respect to $\text{C}=\text{O}$ bond) and the $\text{O}-\text{CH}_3$ bond synperiplanar with respect to the $\text{C}=\text{O}$ bond. The syn form is the preferred form and becomes the exclusive form in the crystalline solid at low temperature. This experimental result is reproduced very well by Hartree–Fock approximation and by density functional theory at different levels of theory but not by the MP2/6-311G* method, which overestimates the value of ΔG° between the syn and anti conformers. The results are discussed in terms of anomeric effects and a natural bond orbital (NBO) calculation. Photolysis of matrix-isolated $\text{CH}_3\text{OC}(\text{O})\text{SCI}$ with broad-band UV–visible irradiation produces an interconversion of the conformers, and the concomitant decomposition leads to formation of OCS and CO molecules.

Introduction

Sulfenyl carbonyl compounds are an interesting family of molecules related to important biological systems such as coenzyme A (CoA). Their properties in the ground and excited electronic states are related to their planar structures and to the syn–anti conformational equilibrium in the gas and liquid phase.

A rather large number of $-\text{C}(\text{O})\text{S}-$ compounds have already

been analyzed with respect to their conformational properties. $\text{FC}(\text{O})\text{SCI}$ was the first example in this series that shows a photolytic interconversion process.¹ Moreover, bond isomerization to $\text{ClC}(\text{O})\text{SF}$ has been observed recently for this compound when it is isolated at low temperatures.²

The syn–anti interconversion process takes place also in $\text{FC}(\text{O})\text{SNSO}_3$ and $\text{FC}(\text{O})\text{SSC}(\text{O})\text{F}$.⁴ $\text{FC}(\text{O})\text{SBr}$ shows similar behavior.⁵ Longer irradiation times lead to the formation of BrSF , which was observed for the first time in this experiment, analogously to the formation of ClSF starting with $\text{FC}(\text{O})\text{SCI}$.⁶ More recently, $\text{ClC}(\text{O})\text{SBr}$ was the subject of

* Corresponding author. CC 962, 1900 La Plata, República Argentina. E-mail: carlosdv@quimica.unlp.edu.ar.

[†] This work is part of the Ph.D. thesis of M.F.E. M.F.E. is a fellow of CONICET. R.M.R. and C.O.D.V. are members of the Carrera del Investigador of CONICET, República Argentina.

[‡] Departamento de Química, Facultad de Ciencias Exactas, Universidad Nacional de La Plata.

[§] Laboratorio de Servicios a la Industria y al Sistema Científico, Universidad Nacional de La Plata.

^{||} Universität GH Essen.

[⊥] Universität Tübingen.

[∇] Universität GH Duisburg.

[∞] Universidade de Sao Paulo.

(1) Mack, H.-G.; Oberhammer, H.; Della Védova, C. O. *J. Phys. Chem.* **1991**, *95*, 4238–4241.

(2) Romano, R. M.; Downs, A. J.; Della Védova, C. O. Unpublished results.

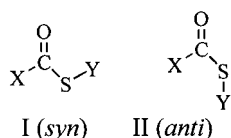
(3) Mack, H.-G.; Oberhammer, H.; Della Védova, C. O. *J. Mol. Struct.* **1992**, *265*, 347–357.

(4) Mack, H.-G.; Oberhammer, H.; Della Védova, C. O. *J. Phys. Chem.* **1992**, *96*, 9215–9217.

(5) Della Védova, C. O.; Mack, H.-G. *Inorg. Chem.* **1993**, *32*, 948–950.

(6) Willner, H. *Z. Naturforsch.* **1984**, *39B*, 314–316.

Chart 1



further investigations.⁷ After broad-band UV–visible photolysis, the novel constitutional isomer *syn*-BrC(O)SCl is observed and subsequently the new triatomic sulfur halide BrSCl.

As described above, the conformers are planar with two potential energy minima (Chart 1), corresponding to the *syn* (I) and *anti* (II) forms.

Several effects can be suggested to rationalize these experimental observations:

(a) Hydrogen bonding. Hydrogen bonding may be operative in compounds such as $\text{FC}(\text{O})\text{SCH}_3$ ^{8–10} and $\text{CF}_3\text{C}(\text{O})\text{SH}$.¹¹ Crowder¹² interpreted the vibrational data of $\text{CF}_3\text{C}(\text{O})\text{SH}$ assuming that the CF_3 group staggers the $\text{C}=\text{O}$ bond, allowing the formation of a planar FCCSH five-membered ring conformation with an estimated $\text{F}\cdots\text{H}$ contact of 2.4 Å. More recent studies¹¹ suggested an eclipsed orientation of this group for the *anti* form with an $\text{F}\cdots\text{H}$ separation of ca. 2.7 Å. Moreover, only the *syn* form was experimentally detected in the gas phase according to gas electron diffraction (GED).

Formation of a cyclic dimer of $\text{CH}_3\text{C}(\text{O})\text{SH}$ is believed to be favored at low temperatures in a mixture of Freon solvents. This clearly indicates intermolecular hydrogen bridges, which must be taken into account in the evaluation of the vibrational spectra of the liquid and of the solid phase.¹³

(b) Lone pair–lone pair repulsion. This family of compounds shows in both conformations lone pair–lone pair repulsions with the exception of the smallest member of this series, $\text{HC}(\text{O})\text{SH}$. It is worth mentioning that $\text{HC}(\text{O})\text{SH}$ adopts mainly the *syn* conformation, but the *anti* form, in which destabilizing interactions between the lone pairs at oxygen and at sulfur occur, is also present in smaller amounts in the gas and liquid phase.^{14,15}

(c) Dipole–dipole interactions. Electrostatic interactions can play a role in the stabilization of *syn* and *anti* forms. This effect could be important in molecules of the type $\text{CH}_3\text{C}(\text{O})\text{SC}(\text{O})\text{CH}_3$. Spectroscopic, X-ray, and electron diffraction results demonstrate that a *syn*–*anti* conformation is the most stable form of this compound.¹⁶

Chart 2

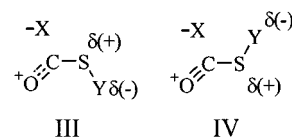
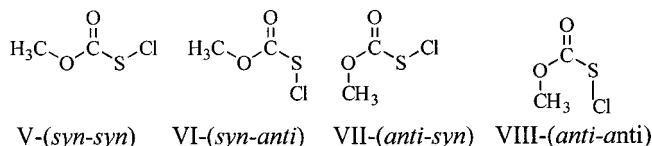


Chart 3



(d) Aromaticity. The stabilization of the *syn* conformer of $\text{FC}(\text{O})\text{SCH}_3$ is accounted for by the attractive π non-bonded interactions in that conformation. Moreover, the absence of any appreciable amount of the *anti* form in this molecule can be understood on the basis of this interaction.

(e) Anomeric effect. If one of the central atoms in an A-B-C-D chain, e.g., B, possesses one or more lone pairs, the generalized anomeric effect may have a large influence on the conformational properties.¹⁷ This effect contributes to the preference for the *syn* form for the conformation of $-\text{C}(\text{O})\text{S}$ -containing compounds.¹⁸

(f) Steric interactions. The expected behavior is observed in $\text{CNC}(\text{O})\text{SCH}_3$ by only steric interaction arguments. Considering that the CN is larger than O, a *syn* form is expected for this molecule.¹⁹ However, steric interactions would favor the *anti* conformation in $\text{HC}(\text{O})\text{SCH}_3$, but only the *syn* form has been detected in the gas phase.²⁰

(g) Mesomeric structures. Mesomeric forms of the $-\text{C}(\text{O})\text{S}$ -containing compounds would explain the higher wavenumbers and related force constants of the *syn* conformer when Y is electronegative and the opposite trend with Y electropositive in $\text{XC}(\text{O})\text{SY}$ compounds. These could be accounted for by stabilization derived from different $\text{C}=\text{O}$ polarizations, as shown in Chart 2.¹⁴

In principle, the title compound can exist in four different conformations (Chart 3) with planar skeleton.

In the present work, the results of a gas electron diffraction analysis, of low-temperature X-ray diffraction, and spectroscopic experiments with $\text{CH}_3\text{OC}(\text{O})\text{S}\text{Cl}$ in the gas phase, in the liquid phase, and isolated in solid Ar at ca. 15 K are reported. Irradiation with broad-band UV–visible light induces the conversion to the *anti* conformer, leading to the spectroscopic characterization of a rotamerization.

Subsequent quantum chemical calculations have been performed for the sake of comparison. Moreover, results are discussed in terms of anomeric effects, using a natural bonding orbital analysis (NBO).

(7) Romano, R. M.; Della Védova, C. O.; Downs, A. J.; Green, T. M. *J. Am. Chem. Soc.* **2001**, *123*, 5794–5801.

(8) Della Védova, C. O. *J. Raman Spectrosc.* **1989**, *20*, 483–488.

(9) Caminati, W.; Meyer, R. *J. Mol. Spectrosc.* **1981**, *90*, 303.

(10) Romano, R. M.; Downs, A. J.; Della Védova, C. O. Unpublished results.

(11) Gobbato, K. I.; Della Védova, C. O.; Mack, H.-G.; Oberhammer, H. *Inorg. Chem.* **1996**, *35*, 6152–6157.

(12) Crowder, G. A. *Appl. Spectrosc.* **1973**, *27*, 440.

(13) Noe, E. A. *J. Am. Chem. Soc.* **1977**, *99*, 2803–2805.

(14) Della Védova, C. O. *J. Raman Spectrosc.* **1991**, *22*, 291–295.

(15) Hocking, W. H.; Winnewisser, G. *Z. Naturforsch.* **1977**, *32A*, 1108.

(16) Romano, R. M.; Della Védova, C. O.; Downs, A. J.; Oberhammer, H.; Parsons, S. *J. Am. Chem. Soc.* **2001**, *123*, 12623–12631.

(17) Kirby, A. J. *The Anomeric Effect and Related Stereoelectronic Effects at Oxygen*; Springer: Berlin, 1983.

(18) Larson, J. R.; Epiotis, N. D.; Bernardi, F. *J. Am. Chem. Soc.* **1978**, *100*, 5713–5716.

(19) Caminati, W. *J. Mol. Spectrosc.* **1981**, *90*, 315.

(20) Caminati, W.; Van Eijck, B. P.; Lister, D. G. *J. Mol. Spectrosc.* **1981**, *90*, 15.

Table 1. Crystallographic Data^a for the Structural Analysis of CH₃OC(O)SCI^b

chemical formula	C ₂ H ₃ ClO ₂ S	crystal system	monoclinic
formula mass	126.55	volume	501.7(2) Å ³
crystallization temp	173(2) K	Z	4
crystal size	0.3 mm diameter	space group	P21/c
unit cell parameters ^c		density (calcd)	1.676 g/cm ³
<i>a</i>	7.7364(18) Å	wavelength	0.71073 Å
<i>b</i>	8.807(2) Å	abs coeff	1.036 mm ⁻¹
<i>c</i>	8.200(2) Å	extinction coeff	0.179(12)
α	90°	μ	1.036 mm ⁻¹
β	116.121(18)°		
γ	90°		
intensities of refln ^d	2.93–30.04°		
reflns collected	1531		
independent reflns ^e	1438		

^a Crystal structure data have been deposited at the Cambridge Crystallographic Data Centre (CCDC). Inquiries for data can be directed to the Cambridge Crystallographic Data Centre, 12 Union Road, Cambridge, U.K. CB2 1EZ, or (e-mail) deposit@ccdc.cam.ac.uk or (fax) +44 (0) 1223 336033. Any request to the CCDC for this material should quote the full literature citation and the reference number 163674. ^b Treatment of hydrogen atoms: riding model on idealized geometries with the 1.5-fold isotropic displacement parameters of the equivalent U_{ij} of the corresponding carbon atom. ^c From diffractometer angles of 50 reflns ($20 \leq 2\theta \leq 25$) refined by least-squares methods. ^d $R(\text{merge}) = 0.0962/0.0646$. ^e $R(\text{int}) = 0.0475$.

Experimental Section

Methoxycarbonylsulphenyl chloride (Aldrich, >97%) was purified by fractional trap-to-trap condensation at 10^{-2} – 10^{-3} Torr, and its purity was checked by IR and ¹H and ¹³C NMR spectroscopy. Infrared spectra between 4000 and 400 cm⁻¹ were recorded on a Bruker IFS 66v Fourier transform instrument with a resolution of 1 cm⁻¹, using a 10-cm gas cell with Si windows. Raman spectra of the liquid substance were measured perpendicular to the incident beam on a Jobin-Yvon U 1000 model (resolution 1 cm⁻¹). The 514.5 nm radiation of an argon ion laser was applied for excitation.

NMR spectra were recorded with a Bruker AC 250 spectrometer and referenced with (CH₃)₄Si as standard in CDCl₃ solutions.

Low-temperature IR spectra of Ar matrixes (sample-to-Ar ratio 1:1000) were taken in a cryogenic system. The mixture was deposited on a metal mirror at ca. 15 K by the continuous deposition technique. For the photochemical study, a Heraeus TQ 150 mercury lamp was employed. The radiation was filtered with water.

An appropriate crystal of CH₃OC(O)SCI was obtained on the diffractometer by a miniature zone-melting procedure with focused infrared light.^{21,22} The diffraction intensities were measured at low temperature on a Nicolet R3m/V four-circle diffractometer. Intensities were collected with graphite-monochromatized Mo K α radiation by the ω -scan technique. The crystallographic data, conditions, and some features of the structure are listed in Table 1. The structure was solved by Patterson syntheses and refined by full-matrix least-squares methods on F with the SHELXTL-Plus program.²³ All atoms with the exception of the hydrogens were assigned anisotropic thermal parameters. Atomic coordinates and equivalent isotropic displacement coefficients are given in Table 2.

(21) Brodalla, D.; Mootz, D.; Boese, R.; Osswald, W. *J. Appl. Crystallogr.* **1985**, *18*, 316.

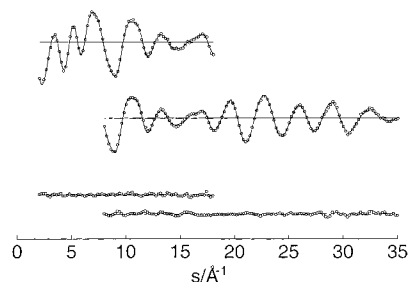
(22) Boese, R.; Nussbaumer, M. In *Situ Crystallisation Techniques*. In *Organic Crystal Chemistry*; Jones, D. W., Ed.; Oxford University Press: Oxford, England, 1994; pp 20–37.

(23) SHELXTL-Plus Version SGI IRIS Indigo, a Complex Software Package for Solving, Refining and Displaying Crystal Structures; Siemens: Germany, 1991.

Table 2. Atomic Coordinates ($\times 10^4$) and Equivalent Isotropic Displacement Parameters ($\text{Å}^2 \times 10^3$) for CH₃OC(O)SCI

	<i>x</i>	<i>y</i>	<i>z</i>	$U(\text{eq})^a$
S(1)	8896(1)	9443(1)	1596(1)	37(1)
Cl(1)	8254(1)	7546(1)	101(1)	50(1)
O(1)	6118(2)	10417(1)	-1548(1)	49(1)
O(2)	7565(1)	12065(1)	771(1)	37(1)
C(1)	6437(2)	13318(2)	-360(2)	41(1)
C(2)	7251(2)	10723(1)	-39(2)	30(1)

^a $U(\text{eq})$ is defined as one-third of the trace of the orthogonalized U_{ij} tensor.

**Figure 1.** Experimental (O) and calculated (—) molecular scattering intensities and differences for CH₃OC(O)SCI.**Table 3.** Calculated Relative Energies^a of syn–syn, syn–anti, and anti–syn Conformers of CH₃OC(O)SCI

method	syn–syn	syn–anti	anti–syn
HF/6-31G*	0.00	1.00	9.56
HF/6-31++G**	0.00	0.90	9.30
HF/6-311++G**	0.00	1.02	9.07
B3LYP/6-31G*	0.00	0.23	7.60
B3LYP/6-31++G**	0.00	0.18	6.61
B3LYP/6-311++G**	0.00	0.35	6.55
B3PW91/6-311++G**	0.00	0.40	6.15
MP2/6-311G*	0.00	1.62	7.33

^a Energies are given in kilocalories per mole.

The GED intensities were recorded with a Gasdiffraktograph KD-G2²⁴ at 25 and 50 cm nozzle-to-plate distances and with an accelerating voltage of about 60 kV. The sample, inlet system, and nozzle (0.6 mm inner diameter) were kept at room temperature. The photographic plates (Kodak Electron Image Plates, 13 × 18 cm) were analyzed with the usual methods.²⁵ Averaged molecular intensities in the *s* ranges 2–8 and 8–35 Å⁻¹, in intervals of $\Delta s = 0.2 \text{ Å}^{-1}$ [$s = (4\pi/\lambda) \sin \theta/2$; λ = electron wavelength, θ = scattering angle], are presented in Figure 1.

Quantum Chemical Calculations. The geometric structure of the syn–syn, syn–anti, and anti–syn conformers were optimized with the Hartree–Fock (HF) approximation and density functional theory (DFT) methods using 6-31++G** basis sets and with the MP2 approximation using 6-311G* basis sets. The anti–anti rotamer does not correspond to a minimum because of steric repulsions. All three stable rotamers possess planar molecular skeletons, and the relative energies obtained with the different methods are given in Table 3. From these values a mixture of syn–syn and syn–anti rotamers is expected, whereas the anti–syn form should not be observable in the experiments. The potential curves for internal rotation around the C(sp²)–S and C(sp²)–O bonds (Figures 2 and 3) were calculated by the B3LYP/6-31++G** method, with structure optimizations for torsional angles performed

(24) Oberhammer, H. *Molecular Structure by Diffraction Methods*; The Chemical Society: London, 1976; Vol. 4, p 24.

(25) Oberhammer, H.; Gombler, W.; Willner, H. *J. Mol. Struct.* **1981**, *70*, 273.

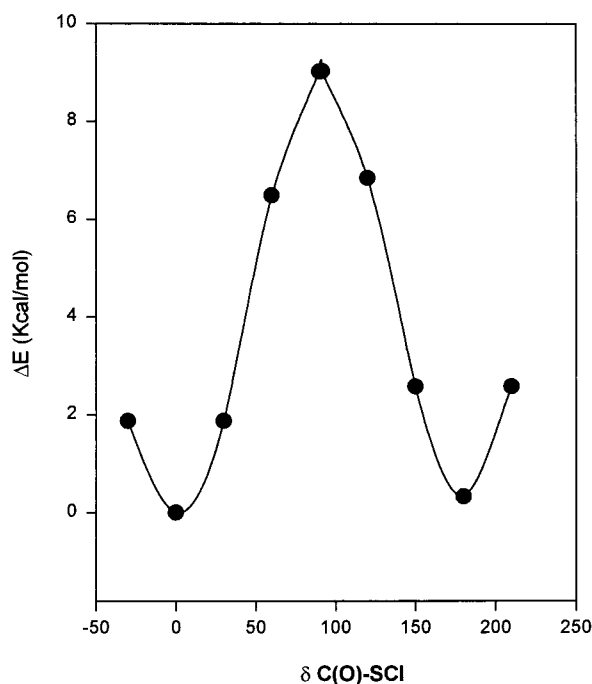


Figure 2. Potential energy curve for $\text{CH}_3\text{OC}(\text{O})\text{Cl}$ as a function of the $\text{C}(\text{O})\text{-S-Cl}$ dihedral angle calculated with B3LYP/6-31++G**.

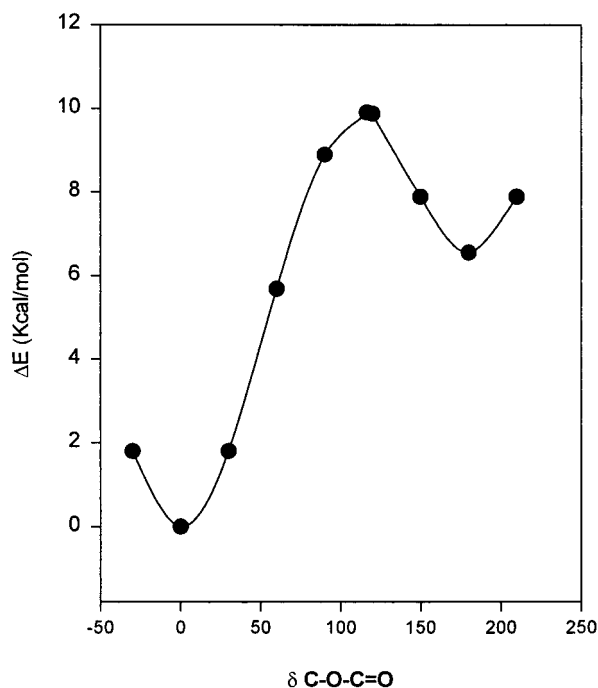


Figure 3. Potential energy curve for $\text{CH}_3\text{OC}(\text{O})\text{Cl}$ as a function of the $\text{C-O-C}(\text{O})$ dihedral angle calculated with B3LYP/6-31++G**.

in steps of 30° . The barriers to internal rotation are 9.0 kcal/mol for the $\text{syn-syn} \rightarrow \text{syn-anti}$ transformation and 9.9 kcal/mol for the $\text{syn-syn} \rightarrow \text{anti-syn}$ transformation. Vibrational wavenumbers for the two low-energy conformers, syn-syn and syn-anti , have been calculated by the B3LYP/6-31++G** method. From the thermodynamic analysis a correction between ΔE and ΔG° of 0.07 kcal/mol has been derived. The vibrational amplitudes were calculated from the Cartesian force constants with the program ASYM40.²⁶ All quantum chemical calculations were performed

with the GAUSSIAN98 program suite²⁷ under the LINDA parallel execution environment.

Crystallographic Studies. The molecular structure of solid $\text{CH}_3\text{-OC}(\text{O})\text{SCl}$ corresponds to the most stable syn-syn form. The geometric parameters are included in Table 4.

Results

Vibrational Analysis. The observed wavenumbers in the IR (gas and matrix) and Raman spectra, together with a tentative assignment and the theoretical wavenumbers (B3LYP/6-31++G**), are collected in Table 5. The $3N - 6 = 21$ normal modes of vibration for $\text{syn CH}_3\text{OC}(\text{O})\text{SCl}$ can be classified as 14 A' in-plane modes and 7 A'' out-of-plane modes in the C_s symmetry group. The more interesting bands in the IR spectra, located at 1779, 1194, 1154, and 558 cm^{-1} , correspond to $\nu_{\text{C=O}}$, $\nu_{\text{OC}(\text{O})}$, δ_{COC} , and $\nu_{\text{S-Cl}}$ modes, respectively. The vibrational assignment was performed by use of the common criteria of relative intensities, depolarization ratios of the liquid Raman bands, evaluation of the gas IR contours, and comparison with related molecules (see Table 5). Subsequent comparison with the theoretical data seems to confirm the proposed assignment.

In the C=O stretching region of the IR(gas) spectrum (Figure 4), two bands are observed. The band contours can be described as B-type for the higher wavenumber absorption and a hybrid AB-type for the lower one. The well-defined rotational contours allow an assignment of these bands to the two conformers. The almost parallel orientation of the carbonyl oscillator with respect to the principal axis of inertia B in the main conformer results in a B-type band. Similarly, a hybrid AB band is expected for the second conformer (Figure 5). The gauche arrangement can be excluded according to the lack of C-type contours of the $\nu_{\text{C=O}}$ band expected for any nonplanar form.

A ratio of areas $A(\text{syn-syn})/A(\text{syn-anti}) = 0.39$ can be obtained from the gas IR spectra of the two carbonyl bands. Since the calculated IR intensities (square of transition moments) of the two conformers are very similar, this ratio corresponds closely to the ratio of the two conformers, leading to $\Delta G^\circ \approx 0.6 \text{ kcal/mol}$. For a quantitative analysis of the conformational composition, a gas/Ar mixture (1:1000) at different temperatures (20, 110, 220, and 330°C) was deposited on the He-cooled copper mirror. The intensity ratio of the anti and syn bands increases with increasing temperature, and $\Delta H^\circ = 0.68(15) \text{ kcal/mol}$ is derived from the van't Hoff plot (Figure 6). From the calculated entropy difference $\Delta S^\circ = -0.28 \text{ cal}/(\text{K}\cdot\text{mol})$, a value of $\Delta G^\circ = 0.76(15) \text{ kcal/}$

(27) Frisch, M. J.; Trucks, G. W.; Schlegel, H. B.; Scuseria, G. E.; Robb, M. A.; Cheeseman, J. R.; Zakrzewski, V. G.; Montgomery, J. A.; Stratman, R. E.; Burant, J. C.; Dapprich, S.; Millam, J. M.; Daniels, A. D.; Kudin, K. N.; Strain, M. C.; Farkas, O.; Tomasi, J.; Barone, V.; Cossi, M.; Cammi, R.; Mennucci, B.; Pomelli, C.; Adamo, C.; Clifford, S.; Ochterski, J.; Petersson, G. A.; Ayala, P. Y.; Cui, Q.; Morokuma, K.; Malick, D. K.; Rabuck, A. D.; Raghavachari, K.; Foresman, J. B.; Cioslowski, J.; Ortiz, J. V.; Stefanov, B. B.; Liu, G.; Liashenko, A.; Piskorz, P.; Komaromi, I.; Gomperts, R.; Martin, R. L.; Fox, D. J.; Keith, T.; Al-Laham, M. A.; Peng, C. Y.; Nanayakkara, A.; Gonzalez, C.; Challacombe, M.; Gill, P. M. W.; Johnson, B.; Chen, W.; Wong, M. W.; Andres, J. L.; Gonzalez, C.; Head-Gordon, M.; Replogle, R. E.; Pople, J. A. GAUSSIAN 98 (Revision A.6); Gaussian, Inc.: Pittsburgh, PA, 1998.

(26) Hedberg, L.; Mills, I. M. *J. Mol. Spectrosc.* **1993**, *160*, 117.

Table 4. GED, X-ray, and Calculated Geometric Parameters for syn–syn CH₃OC(O)SCL^a

parameter	GED ^b		X-ray	MP2/ 6-311G*	B3LYP/ 6-31++G**	HF/ 6-31++G**
C–H	1.093(16)	p1		1.089	1.089	1.079
C=O	1.185(3)	p2	1.1902(16)	1.199	1.202	1.178
(O–C)mean	1.381(4)	p3		1.391	1.395	1.371
ΔOC ^c	0.103[10] ^d			0.103	0.108	0.116
O2–C1	1.329(7)		1.3249(16)	1.340	1.341	1.313
O2–C2	1.432(7)		1.4587(17)	1.443	1.449	1.428
C–S	1.778(4)	p4	1.7846(13)	1.792	1.811	1.786
S–Cl	1.999(2)	p5	2.0006(7)	2.042	2.057	2.017
O1=C1–O2	129.1(7)	p6	127.69(12)	127.5	127.3	126.9
O1=C–S	126.1(7)	p7	126.40(11)	127.5	127.2	126.5
C1–O2–C2	114.3(10)	p8	115.49(10)	113.5	115.8	117.2
C1–S–Cl	99.1(3)	p9	99.46(5)	99.2	100.3	101.0
H–C–H	111.1(34)	p10		110.6	110.0	108.4
tilt(CH ₃)	3.3 ^e			3.3	4.2	3.5
δ(C–O–C=O)	0.0 ^e		–2.86(0.21)	0.0	0.0	0.0
δ(C–O–C–S)	180.0 ^e		176.82(0.09)	180.0	180.0	180.0
δ(Cl–S–C=O)	0.0 ^e		1.43(0.14)	0.0	0.0	0.0
δ(Cl–S–C–O)	180.0 ^e		–178.25(0.08)	180.0	180.0	180.0
%(syn–anti) ^f	28(8)			6	41	18
ΔG ^g (kcal/mol)	0.57(19)			1.62	0.21	0.89

^a Values are given in angstroms and degrees. For atom numbering see Figure 8. ^b r_a values with 3σ uncertainties in parentheses. ^c ΔOC = (O2–C2) – (O2–C1). ^d MP2 value with estimated uncertainty in brackets. ^e Not refined. ^f %(syn–anti) represents the concentration of the less stable syn–anti form, syn with respect to the H₃C–O bond and the C=O double bond and anti with respect to the S–Cl bond and the C=O double bond.

Table 5. Experimental and Theoretical Vibrational Data and Assignment of the Vibrational Modes for CH₃OC(O)SCL

mode	B3LYP/6-31++ G**(intensities)		IR (gas) ^a		Raman (liq) ^b		IR (Ar matrix)		assignment ^c (symmetry)
	syn–syn	syn–anti	syn	anti	syn	anti	syn	anti	
ν_1	3191 (13)	3195 (7)	3014vw		3039				$\nu_{\text{C–H}}(\text{A}')$
ν_2	3073 (29)	3076 (26)	2850vw		2840				$\nu_{\text{C–H}}(\text{A}')$
ν_3	1821 (284)	1772 (306)	1779s	1733m	1756p	1712	1772 ^d	1723	$\nu_{\text{C=O}}(\text{A}')$
ν_4	1499 (13)	1497 (11)	1454vw				1465	1453	$\delta_{\text{CH}_3}(\text{A}')$
ν_5	1488 (10)	1489 (10)	1302vw		1329		1435	1428	$\delta_{\text{CH}_3}(\text{A}')$
ν_6	1211 (193)	1232 (513)	1194s		1196p		1190	1208	$\rho_{\text{CH}_3}(\text{A}')$
ν_7	1179 (544)	1169 (1)	1154vs				1151		$\delta_{\text{COC}}(\text{A}')$
ν_8	963 (3)	976 (9)	977vw		937p	955	954		$\nu_{\text{OC}}(\text{A}')$
ν_9	812 (38)	824 (33)	813w		816p		812		$\delta_{\text{O–C(O)}}(\text{A}')$
ν_{10}	534 (21)	513 (35)	558w		555p	547			$\nu_{\text{S–Cl}}(\text{A}')$
ν_{11}	481 (1)	448 (1)			489p	545			$\nu_{\text{S–C}}(\text{A}')$
ν_{12}	351 (20)	361 (5)			363p	374			$\nu_{\text{COC}}(\text{A}')$
ν_{13}	260 (8)	268 (16)			274p	290			$\delta_{\text{COCH}_3}(\text{A}')$
ν_{14}	143 (1)	152 (4)			155p				$\delta_{\text{OC(O)}, \delta_{\text{CSCl}}}(\text{A}')$
ν_{15}	3159 (13)	3163 (12)	2966w		2959				$\nu_{\text{C–H}}(\text{A}'')$
ν_{16}	1470 (11)	1470 (17)	1437w				1450	1436	$\delta_{\text{CH}_3}(\text{A}'')$
ν_{17}	1168 (1)	1197 (116)		1159sh	1153dp			1180	$\rho_{\text{CH}_3}(\text{A}'')$
ν_{18}	661 (10)	663 (12)	666vw		664dp		661		$\rho_{\text{OPOC(O)S}}(\text{A}'')$
ν_{19}	139 (3)	130 (2)							$\rho_{\text{H3C–O(asym)}}(\text{A}'')$
ν_{20}	106 (2)	112 (1)							$\rho_{\text{H3C–O(sym)}}(\text{A}'')$
ν_{21}	82 (1)	88 (0.3)				77			$\tau_{\text{CO–C(O)}}(\text{A}'')$

^a vs, very strong; s, strong; m, medium; w, weak; vw, very weak. ^b p, polarized; dp, depolarized. ^c ν , δ , τ and ρ represent stretching, deformation, torsion, and rocking modes. ^d Split in two peaks due to matrix effect.

mol is derived. From the temperature dependence (–50, –20, 0, 20, and 50 °C) of the Raman spectra, $\Delta H^\circ = 0.43(4)$ kcal/mol has been derived for the liquid state from the van't Hoff plot (Figure 7). According to these values, intermolecular interactions seem to favor the second conformation in the liquid with respect to the gas phase. These interactions are responsible for the shift of the C=O stretching wavenumbers when going from the gas phase to the liquid in all -C(O)S-containing compounds that have been studied.

Gas-Phase Structure. The experimental radial distribution function (RDF) derived by Fourier transformation of the molecular intensities is compared to RDFs calculated for syn–syn and syn–anti conformations in Figure 8. The two calculated curves differ strongly in the range of the first

nonbonded distances (2.2–3.2 Å), reflecting large changes of bond angles between the syn–syn and syn–anti forms (see below). Furthermore, the RDF for the syn–syn form possesses a peak at 5.2 Å that corresponds to the C2–Cl distance, whereas no interatomic distance longer than 5 Å occurs in the syn–anti conformer. Analysis of the RDF leads to a contribution of about 25% syn–anti form. The geometric parameters of the syn–syn conformer were refined by least-squares fitting of the molecular intensities. The following assumptions were made in this analysis: (i) The CH₃ group was constrained to C_{3v} symmetry and the tilt angle between the C_3 axis and the O–C bond direction was set to the calculated value. (ii) The difference between the O–C bond lengths, ΔCO, was set to the MP2 value. The estimated

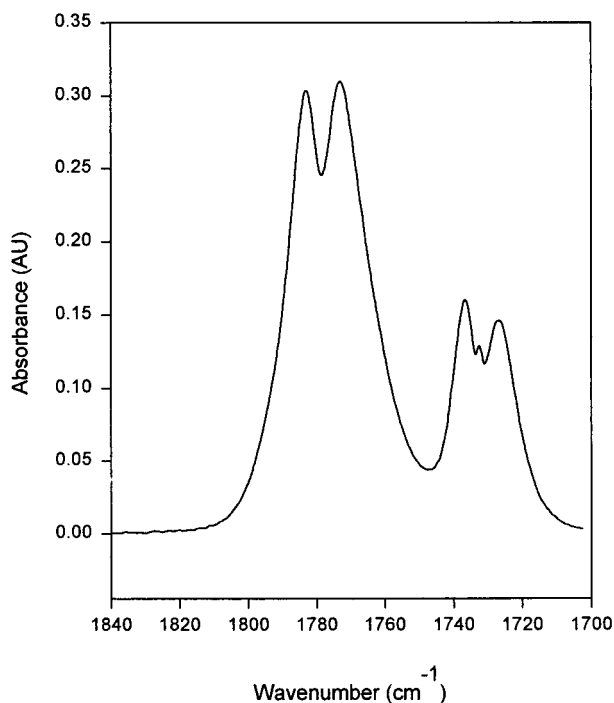


Figure 4. Gas IR carbonylic stretching $\text{C}=\text{O}$ bands of $\text{CH}_3\text{OC}(\text{O})\text{SCl}$ at 8 mbar.

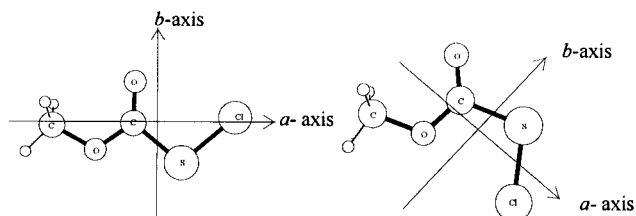


Figure 5. Main moments of inertia (a and b) for the syn and anti conformers of $\text{CH}_3\text{OC}(\text{O})\text{SCl}$ (the c axis is perpendicular to the symmetry molecular plane).

uncertainty of $\pm 0.010 \text{ \AA}$ is taken into account in the uncertainties of the individual $\text{O}-\text{C}$ bond lengths. (iii) Vibrational amplitudes that either cause large correlations between geometric parameters or are poorly determined in the GED experiment are constrained to calculated amplitudes. (iv) The geometric parameters of the syn-anti conformer were tied to those of the syn-syn form, by use of the calculated (MP2) differences. Whereas bond lengths of the two rotamers differ by 0.010 \AA or less, some angles change considerably. The $\text{O}=\text{C}-\text{S}$ angle decreases by 9.8° and the $\text{C}-\text{S}-\text{Cl}$ angle increases by 5.6° if the $\text{S}-\text{Cl}$ bond is rotated from the syn to anti orientation. Calculated vibrational amplitudes were used for the anti conformer. With the above assumptions, 10 geometric parameters ($p1-p10$) and 10 vibrational amplitudes ($l1-l10$) were refined simultaneously. Least-squares refinements with different conformer ratios were performed and the lowest R value was obtained for 28(8)% syn-anti form. The uncertainty is derived with Hamilton's test based on 1% significance.²⁸ The following correlation coefficients had values larger than $|0.5|$: $p3/p8 = -0.53$, $p6/p7 = -0.90$, $p1/l1 = 0.54$, $p9/l7 = 0.56$, $l4/l5$

(28) Hamilton, W. *Acta Crystallogr.* **1965**, *18*, 502.

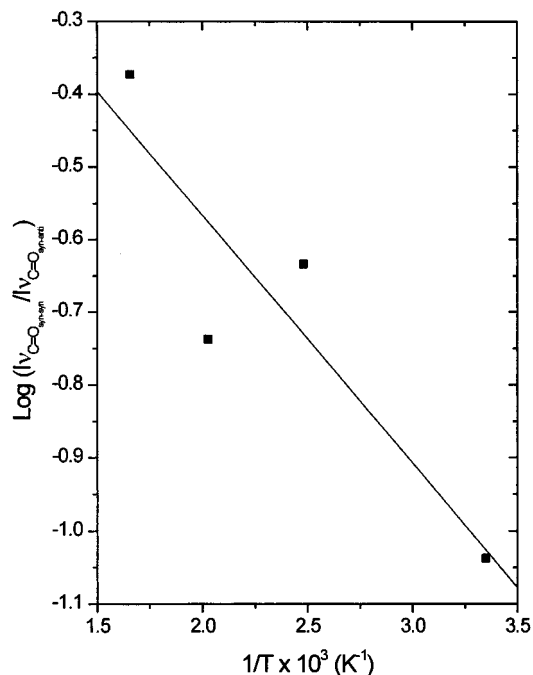


Figure 6. Van't Hoff plot for the $\nu_{\text{C}=\text{O}}$ absorption bands of $\text{CH}_3\text{OC}(\text{O})\text{SCl}$ in matrix-isolated IR experiences.

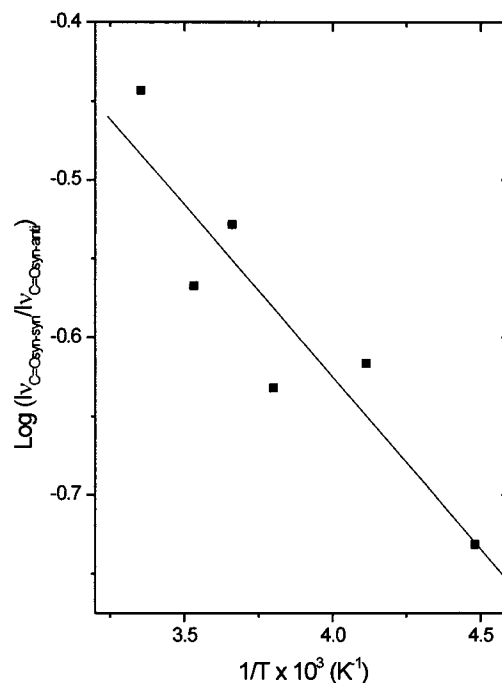


Figure 7. Van't Hoff plot for the liquid Raman $\nu_{\text{C}=\text{O}}$ bands of $\text{CH}_3\text{OC}(\text{O})\text{SCl}$.

$= 0.58$, and $l8/l9 = 0.59$. The geometric parameters are included in Table 4 and the vibrational amplitudes in Table 6.

Matrix Photoisomerization Experiments. As mentioned before, two bands are found in the carbonyl stretching region at 1772 and 1723 cm^{-1} in the IR spectra of the matrix-isolated compound, corresponding to the syn-syn and syn-anti forms, respectively. As shown in Figure 9, if the matrix is irradiated with broad-band UV-visible light, a change occurs with photolytically induced interconversion of the two

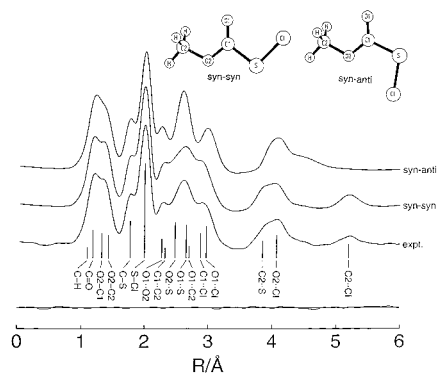


Figure 8. Calculated radial distribution function (RDF) for anti and syn forms of $\text{CH}_3\text{OC}(\text{O})\text{SCL}$ and experimental and difference curves for the mixture [$\text{RDF}(\text{exp}) - \text{RDF}(\text{calc})$]. Molecular models show the syn and anti conformers. Interatomic distances of the syn structure are indicated by vertical bars.

Table 6. Interatomic Distances and Experimental and Calculated (B3LYP/6-31++G**) Vibrational Amplitudes for $\text{CH}_3\text{OC}(\text{O})\text{SCL}^a$

	distance (Å)	expt ^b	calc		distance (Å)	expt ^b	calc
C—H	1.09	0.076 ^c	0.076	O2...S	2.48	0.071(6)	14 0.069
C=O	1.19	0.033(5)	0.037	O1...S	2.64	0.070(7)	15 0.059
O2—C1	1.33	0.045 ^c	0.045	O1...C2	2.69	0.098 ^c	0.089
O2—C2	1.43	0.049 ^c	0.049	C1...Cl	2.89	0.081(13)	16 0.086
C—S	1.78	0.055(4)	0.053	O1...Cl	2.97	0.123(12)	17 0.131
S—Cl	2.00	0.048(2)	0.048	C2...S	3.84	0.083(13)	18 0.071
O1...O2	2.27	0.051 ^c	0.051	O2...Cl	4.07	0.094(11)	19 0.076
C1...C2	2.32	0.065 ^c	0.065	C2...Cl	5.20	0.111(18)	110 0.101

^a Vibrational amplitudes are given without nonbonded distances involving hydrogen atoms. For atom numbering see Figure 8. ^b Experimental uncertainties are 3σ values. ^c Not refined.

conformers, leading to an increase in the intensity of the carbonyl stretching band corresponding to the syn-anti form and to a decrease in the intensity of the corresponding band of the syn-syn form.

Longer irradiation times lead to decomposition with the formation of OCS and CO. In addition, a band corresponding to HCl can be observed, probably being associated with the formation of an adduct with H_2CO .

Discussion

Infrared spectra of the vapor and of Ar matrixes, as well as GED, show the presence of a mixture of syn-syn and syn-anti rotamers in gaseous $\text{CH}_3\text{OC}(\text{O})\text{SCL}$. The contribution of the higher energy syn-anti form is about 25%. According to the Raman spectra, such a mixture with a similar composition is present also in the liquid phase. According to X-ray diffraction at low temperature, only the syn-syn form is present in the crystal. The difference in Gibbs free energy derived from the IR(matrix) spectra [$\Delta G^\circ = 0.76(15)$ kcal/mol] agrees with the value obtained from the GED experiment [$\Delta G^\circ = 0.57(19)$ kcal/mol] within the experimental uncertainties. The mean value of the two experiments is $0.67(24)$ kcal/mol. The calculated energy difference ΔE between the syn-syn and syn-anti forms depends on the computational method (Table 1). According to DFT calculations, ΔE and ΔG° differ by less than 0.1 kcal/mol. Whereas the HF approximation predicts energy differences that are slightly too large, DFT calculations lead

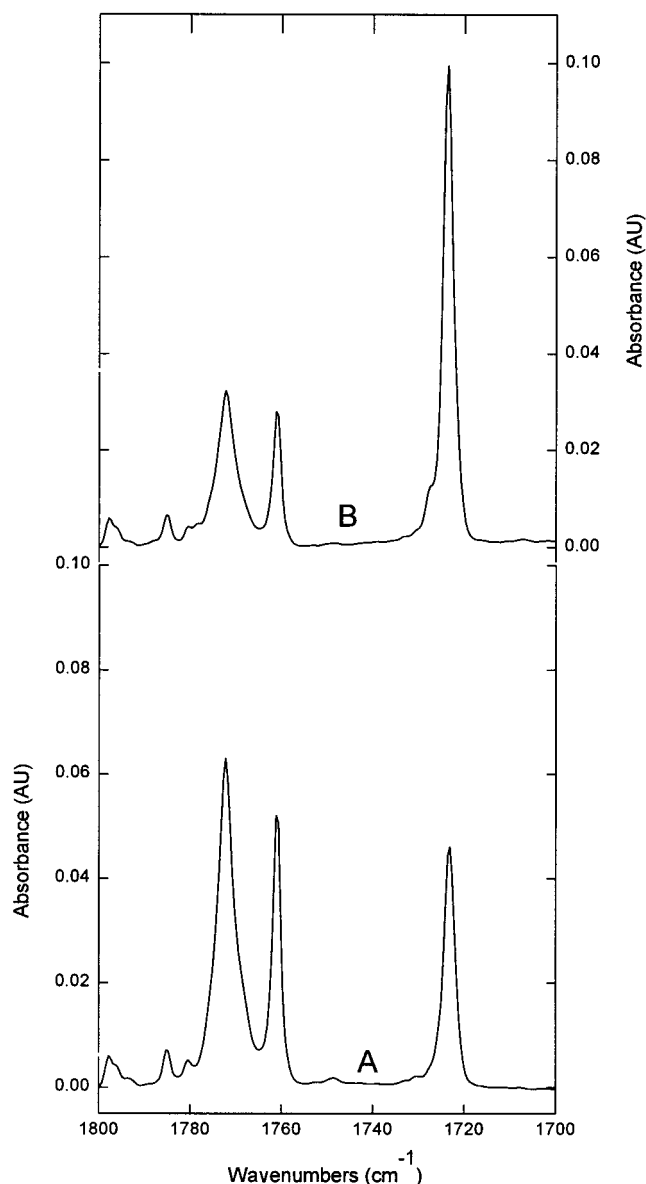


Figure 9. Ar matrix FTIR spectra of $\text{CH}_3\text{OC}(\text{O})\text{SCL}$ (1:1000) in the carbonylic stretching region. (A) Before UV irradiation; (B) after 1 h of UV broad-band irradiation.

to values that are somewhat too small. The value obtained with the MP2 method is definitely too large. In the series of the sulfonyl carbonyl chlorides, $\text{XC}(\text{O})\text{SCL}$, whose conformational properties have been studied, the methoxy derivative ($\text{X} = -\text{OCH}_3$) possesses the lowest energy difference between the anti and syn rotamers (anti/syn refers now to the orientation of the S—Cl relative to the C=O bond). The experimental $\Delta G^\circ = G^\circ(\text{anti}) - G^\circ(\text{syn})$ values increase from $0.67(24)$ to $1.2(3)$ to ca. 1.6 kcal/mol for $\text{Y} = \text{OMe}$, F, and Cl. This trend is reproduced correctly by DFT calculations (B3LYP/6-31++G*), which predict ΔE values of 0.1, 1.0, and 2.6 kcal/mol for the above series. The predicted value for $\text{CF}_3\text{C}(\text{O})\text{SCL}$ for which no anti form was observed experimentally is 3.0 kcal/mol. We may attempt to rationalize these substituent effects on the basis of a natural bond orbital (NBO) analysis. The most important orbital interactions relevant to the conformational properties occur between the

Chart 4

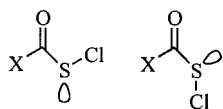


Table 7. Stabilization Energies^a for Orbital Interactions between lp_{π} and lp_{σ} Sulfur Lone Pairs with $\pi^*(C=O)$, $\sigma^*(C=O)$, and $\sigma^*(C-X)$ for syn and anti Conformers and Relative Total Energies for the Series of XC(O)SCI Compounds Using the B3LYP/6-31+G* Approximation

	-F	-Cl	-Br	-CF ₃	-OCH ₃
$lp_{\pi}(S) \rightarrow \pi^*(C=O)$	syn 28.32, anti 28.01	syn 30.30, anti 27.50	syn 31.38, anti 27.55	syn 29.90, anti 29.14	syn 24.39, anti 25.19
$lp_{\sigma}(S) \rightarrow \sigma^*(C=O)$	syn 5.8	syn 5.93	syn 6.14	syn 4.65	syn 5.28
$lp_{\sigma}(S) \rightarrow \sigma^*(C-X)$	anti 3.3	anti 4.38	anti 4.84	anti 2.05	anti 3.08
$\Delta E_{\text{anom}}^{\text{int}b}$	2.5	1.55	1.30	2.60	2.20
$\Delta E_{\text{conj}}^{\text{int}c}$	0.31 (11.2)	2.80 (12.5)	4.03 (13.8)	0.76 (11.7)	-0.80 (9.0)
$\Delta E_{\text{total}}^{\text{int}d}$	2.81	4.35	5.33	3.36	1.40
ΔE^e	1.01	2.64	3.78	3.05	0.12

^a Energies are given in kilocalories per mole. ^b $\Delta E_{\text{anom}}^{\text{int}}$ = Anomeric interaction energy difference of the syn and anti conformers. ^c $\Delta E_{\text{conj}}^{\text{int}}$ = Conjugation interaction energy difference of the syn and anti conformers. Calculated syn-anti rotational barriers are given in parentheses. ^d $\Delta E_{\text{total}}^{\text{int}}$ = $\Delta E_{\text{anom}}^{\text{int}}$ + $\Delta E_{\text{conj}}^{\text{int}}$. ^e $\Delta E = E^{\text{syn}} - E^{\text{anti}}$ is the energy difference of the syn and anti conformers.

two sulfur lone pairs, $lp_{\sigma}(S)$ and $lp_{\pi}(S)$, and the XC(O) moiety (Chart 4). The strongest interaction is that between $lp_{\pi}(S)$ and the $\pi^*(C=O)$ bond [$lp_{\pi}(S) \rightarrow \pi^*(C=O)$], which leads to planar structures for both conformers [also described as the mesomeric effect (conjugation)]. Naively, one would expect that this interaction does not depend on the conformation. The NBO analysis for a series of XC(O)SCI compounds (Table 7) shows, however, that the energy of this orbital interaction varies by up to 4.0 kcal/mol, and therefore, it has to be taken into account. It is worth noting that the calculated $lp_{\pi}(S) \rightarrow \pi^*(C=O)$ interaction energies correlate, as expected, with the calculated torsional barriers, as listed in Table 7. The $lp_{\sigma}(S)$ lone pair can interact either with the $\sigma^*(C=O)$ in the syn form or with the $\sigma^*(C-X)$ orbital in the anti form (anomeric effect). The sum of these orbital interaction energies favors the syn form by 2.8, 4.3, 5.3, 1.4, and 3.4 kcal/mol for the series Y = F, Cl, Br, OMe, and CF₃ and parallels approximately the energy differences between the two conformers.

With due allowance for the systematic differences between GED and X-ray crystallography due to different vibrational effects and/or packing effects in the crystal, the geometric parameters obtained for the gas phase and for the crystal

are in good agreement. The quantum chemical calculations listed in Table 2 reproduce all bond lengths and angles satisfactorily except for the S-Cl bond length, which is predicted to be too long by 0.04–0.06 Å with the MP2 and B3LYP methods. Comparison of the experimental and calculated vibrational wavenumbers (Table 5) shows that the B3LYP method with a large basis set reproduces the experimental wavenumbers very well.

Conclusion

According to GED, vibrational spectroscopy, and ab initio calculations, CH₃OC(O)SCI exists in the gas phase as a mixture of two conformers. The experiments result in a predominance (about 75%) of the syn conformer (carbonyl C=O bond syn with respect to the S-Cl bond). This behavior can be rationalized on the basis of anomeric and mesomeric effects deduced through a natural bond analysis, for the series of related compound FC(O)SCI, ClC(O)SCI, BrC(O)SCI, CH₃OC(O)SCI, and CF₃C(O)SCI. The predominance of the syn form is less marked in the liquid phase, as a result of intermolecular interactions. The X-ray crystallographic studies result in structural parameters of the syn conformer in good agreement with the GED and theoretical ones. If the matrix-isolated CH₃OC(O)SCI is irradiated with broad-band UV-visible light, a change occurs in the relative concentrations of the syn and anti forms due to a photolytic interconversion process.

Acknowledgment. The Argentinean authors thank the Fundación Antorchas, Alexander von Humboldt Stiftung, and DAAD (Deutscher Akademischer Austauschdienst, Germany) for financial support and for the DAAD–Antorchas and von Humboldt–Antorchas Awards to the German–Argentine cooperation. They also thank Professor Dr. P. J. Aymonino (Lanail EFO) for his valuable cooperation, and the Consejo Nacional de Investigaciones Científicas y Técnicas (CONICET), the Comisión de Investigaciones Científicas de la Provincia de Buenos Aires (CIC), República Argentina. They are indebted to the Facultad de Ciencias Exactas, Universidad Nacional de La Plata, República Argentina, for financial support and to the Fundación Antorchas for the National Award to the Argentinean cooperation.

IC010748Y